Check for updates

Immune cell single-cell RNA sequencing analyses link an age-associated T cell subset to symptomatic benign prostatic hyperplasia

Meaghan M. Broman[1], Nadia A. Lanman[1,2], Renee E. Vickman[3,4], Gregory M. Cresswell[1†], Harish Kothandaraman[1], Andree Kolliegbo[5], Juan Sebastian Paez Paez[2,6†], Alexander P. Glaser[3,4], Brian T. Helfand[3,4], Gervaise Henry[7†], Douglas W. Strand[7], Omar E. Franco[8], Simon W. Hayward[3,4] and Timothy L. Ratliff[1,2]*

[1]Department of Comparative Pathobiology, Purdue University, West Lafayette, IN, United States, [2]Purdue Institute for Cancer Research, Purdue University, West Lafayette, IN, United States, [3]Department of Surgery, Endeavor Health formerly NorthShore University HealthSystem, Evanston, IL, United States, [4]Division of Urology, Department of Surgery, University of Chicago Pritzker School of Medicine, Chicago, IL, United States, [5]Department of Computer Science, Purdue University, West Lafayette, IN, United States, [6]Department of Medicinal Chemistry and Molecular Pharmacology, Purdue University, West Lafayette, IN, United States, [7]Department of Urology, University of Texas Southwestern Medical Center, Dallas, TX, United States, [8]Department of Biochemistry and Molecular Biology, Feist-Weiller Cancer Center, Louisiana State University Shreveport, Shreveport, LA, United States

Introduction: Benign prostatic hyperplasia (BPH) is among the most common age-associated diseases in men. Prostatic immune cell infiltration is frequently observed with aging coincident with BPH; however, the contribution of age-related changes in immune cells to BPH is not clear. As T cells are the predominate immune cell in aged prostates, it is hypothesized that age-associated alterations in T cell subsets contribute to BPH symptoms.

Methods: scRNA-seq data from immune cells isolated from small (≤40g) and large (≥90g) prostates from aged men (>50 years) were combined with previously published scRNA-seq data from three young organ donor prostates to compare young to aged prostate T cells and small to large aged prostate T cells. Cycling and senescent BPH patient-derived fibroblasts were treated with granzyme K and senescence-associated secretory phenotype (SASP)-associated cytokines were measured by ELISA.

Results: An age-associated CD8+ T cell subset (Taa) with high Granzyme K (GZMKhi) and low Granzyme B (GZMBlow) gene expression infiltrated aged human prostates and positively correlated with International Prostate Symptom Score (IPSS). A velocity analysis indicated that CD8+ T cell differentiation is altered in large BPH prostates compared to small age-matched prostates, favoring Taa accumulation. In vitro granzyme K treatment of human BPH patient-derived large prostate fibroblasts increased secretion of pro-inflammatory senescence-associated secretory phenotype (SASP)-associated cytokines.

Discussion: These data suggest that granzyme K-mediated stimulation of prostate stromal fibroblast SASP cytokine and chemokine production promotes prostate immune cell recruitment and activation. Overall, these results connect symptomatic BPH with immune aging.

Introduction

Aging is associated with changes in both innate and adaptive immunity collectively referred to as immunosenescence, involving alterations in leukocyte function and increase, an individual's susceptibility to a variety of chronic diseases, infections, and autoimmunity (1–3). While immunosenescence encompasses both adaptive and innate immunity, alterations in the adaptive immune system are a key component in the dysregulated immune response in aged individuals (4, 5). Immunosenescence includes a chronic low-grade inflammation, referred to as inflammaging, that occurs in the absence of pathogens and has been implicated in a variety of age-associated chronic conditions including cardiovascular disease, type 2 diabetes mellitus, obesity, and cancer (1, 6–9). In addition to changes in immune cells, various other cell types and cellular processes may contribute to the chronic inflammation of inflammaging, including the presence of senescent cells in the microenvironment (1, 2, 10, 11). Characteristics of senescent cells include cell cycle arrest, resistance to apoptosis, and a senescence-associated secretory phenotype (SASP), characterized by the production of various cytokines, chemokines and growth factors that promote an inflammatory microenvironment (2, 12). Reduced

removal and accumulation of these senescent cells with age is one consequence of immunosenescence (13).

Among the most common age-related conditions in men is benign prostatic hyperplasia (BPH), affecting approximately half of men over age 50 and nearly 80% by age 80 (14–16). As men age, progressive nodular expansion of both the epithelial and fibromuscular stromal tissues of the prostatic transitional zone (TZ) adjacent to the urethra results in lower urinary tract symptoms (LUTS) (14–18). This expansion is commonly accompanied by immune cell infiltrates that progressively accumulate over time (19). While the underlying cause of BPH and its connection with aging is uncertain, proposed mechanisms include altered androgen levels, prostatic cellular senescence, and changes in immune responses (20–22). Previous studies have associated high prostate inflammatory cell infiltration with increased International Prostate Symptom Score (IPSS) and LUTS (15, 23). Also, prostatitis has been associated with a higher risk of developing BPH-associated LUTS as well as with an increased likelihood of eventually requiring medical or surgical treatment to manage these symptoms (24). Furthermore, immune cell-derived proteins, including pro-inflammatory cytokines, chemokines, and granzymes, have been shown to promote stromal and epithelial cell activation and proliferation as well as exacerbate immune cell recruitment (25–32). These findings led to the hypothesis that age-associated alterations in the prostate immune microenvironment may underlie the development and progression of clinical symptoms of BPH (27, 33, 34). However, the potential contributions of specific immune cell populations and their cellular products to BPH symptoms and progression have not been defined (19, 23, 34, 35).

Other age-associated inflammatory conditions including diabetes, metabolic syndrome, and obesity have been implicated as risk factors for BPH and LUTS (36–38). Additionally, the risk of autoimmune conditions such as rheumatoid arthritis (RA) is increased with age (39), and previous studies have indicated an association between systemic autoimmune inflammation and BPH (40). In all, these studies suggest a role for systemic age-associated immune dysregulation in BPH. Given the T cell dominance of inflammation in the aged prostate (15, 40, 41), we hypothesized that age-associated T cell subpopulations contribute to BPH symptoms. To address this hypothesis, we utilized single-cell RNA-sequencing (scRNA-Seq) to define and compare the immune cells between aged and young normal prostates and between large and small age-

matched prostates to identify potential age-related immune mechanisms of BPH. The results of this study suggest that an age-associated $CD8^+GZMK^{hi}GZMB^{low}$ T cell (Taa) subset contributes to BPH symptoms.

Methods

Human prostate samples

Prostatic tissues were obtained as previously described (40–42). Clinical data for BPH patients is summarized in (41). All human tissue procurement was done with informed consent in accordance with protocols approved by the Institutional Review Boards of each institution.

BPH tissue processing for scRNA-seq

Normal prostate tissues were processed for scRNA-Seq as described (42). For aged prostate tissues, transitional zone (TZ) tissue was excised from each collected large and small prostate and processed as described (40, 41).

Sample sequencing and data analysis

Sequencing of normal prostate cells was performed as described in Henry et al. (42) and is accessible through GEO SuperSeries GSE120716 (42). Sequencing of aged prostate cells was performed as described (40, 41). The aged prostate data is available through GEO under accession number GSE269205. For comparison of aged prostate to normal young prostate immune cells, published scRNA-seq data generated from immune cells isolated from 13 aged (61–76 years) prostate specimens was combined with previously published scRNA-seq data generated from 3 normal prostates obtained from healthy organ donors aged 18–31 years with no reported comorbidities (42). For comparison of large and small aged prostate immune cells, published $CD45^+$ leukocyte scRNA-seq data from the 10 large (51–76 years) and 10 small (63–76 years) aged prostates were used (40, 41). Clustering and subclustering of cells was performed as described (40, 41).

Clinical correlation

Cellular proportions for each cluster and subcluster were computed for each sample. A permutation test was used to calculate a p-value for each cluster, utilizing bootstrapping to calculate the confidence interval for the magnitude of difference between large and small prostates from aged men and young normal prostates. Spearman correlations were computed and statistically significant correlations identified (adjusted p-value < 0.05) between cellular proportions and patient body mass index

(BMI), IPSS, and prostate volume using the corrplot R package version 0.92.

Velocity analysis

The package Velocyto (43) v. 0.17.17 was used to count spliced and unspliced abundances from the CellRanger output BAM files and write these abundances to loom files. The metadata, which includes sample numbers, genes post-filtering, cells post-filtering, embedding coordinates of cells, and clusters were output from Seurat (44) v3 and used in the RNA velocity analysis. Next, scVelo (45) v. 2.4.0 was used to estimate RNA velocity using a likelihood-dynamical model. This dynamical model allows the estimation of RNA velocity even if there is not steady state observed for a given gene, provided that enough spliced and unspliced counts are observed.

Prostate immunofluorescence

Full thickness cross sections of prostate were fixed in 10% neutral buffered formalin (NBF) for histology. Formalin fixed prostate tissues were embedded in paraffin and sectioned. Sections were deparaffinized and blocked with 2.5% Normal Goat serum for 20 minutes. Sections were incubated with primary antibodies for CD8a (clone C8/144B, Abcam) at 1:100 and Granzyme K (polyclonal, Novus Biologicals) at 1:50 for 60 minutes the rinsed twice with staining buffer. The sections were incubated with GoRb488 at 1:250 and GoM555 at 1:500 for 30 minutes then rinsed once with buffer. Sections were counterstained with DAPI for 15 minutes and rinsed with water before applying Prolong Gold mounting media and coverslipping. Stained slides were digitized using a Leica Versa8 whole-slide scanner (Leica, Wetzlar, Germany) and analyzed using the Visiopharm digital slide analysis platform (Visiopharm, Hørsholm, Denmark).

Aged prostate bulk RNA-seq

Frozen TZ tissue from 10 small and 7 large prostates from the same patient cohort as the aged prostate scRNA-seq analysis were placed in Trizol and homogenized using a tissue shredder. After isolation of RNA following the Trizol protocol, cleanup was conducted using the RNeasy Plus mini kit (Qiagen). RNA concentration and quality were determined using a Nanodrop 2000 spectrophotometer (ThermoFisher) and Qubit 4 fluorometer using RNA BR reagents (Invitrogen). RNA was sent to Novogene Corporation Inc. for quality control and strand-specific cDNA library preparation. Bulk RNA-seq paired-end 150 bp reads were sequenced by Novogene. STAR aligner v2.6.1d (46) was used to align reads to the human reference genome, allowing 2 mismatches, and FeatureCounts v1.5.0-p3 (47) was used with default parameters to generate the count matrix. DESeq2 v1.20.0 (48) was used to

identify differentially expressed genes (padj<0.05). Bulk RNA-seq data is accessible through GEO under the accession number GSE295879.

BPH prostate fibroblast and T cell scRNA-seq analysis

Previously published scRNA-seq data generated from all viable cells following tissue digests of 5 large prostate TZ obtained from patients aged 59–73 years undergoing simple prostatectomy surgery for symptomatic BPH was used to analyze BPH T cells and fibroblasts (40). Both raw and processed scRNA-seq data are available on GEO under accession number GSE183676.

Rheumatoid arthritis T cell analysis

To compare the BPH T cell subset to rheumatoid arthritis-derived T cell subsets, we trained a classifier based on T cell subset marker genes from the Supplementary Data from Zhang et al. (49). The top 20 genes identified for the T cell subsets CCR7+(SC-T1), Treg (SC-T2), Tph and Tfh (SC-T3), GZMK+(SC-T4), CTLs (SC-T5), and GZMK+GZMB+ (SC-T6) T cells were used as input into Garnett (49, 50). The Garnett classifier was trained using default parameters and then classified our cells with the resulting model using default parameters.

Human BPH fibroblast culture and cytokine analysis

Human prostate fibroblasts were obtained from the freshly isolated transition zones of 2 BPH patient specimens following simple prostatectomy surgery. Fibroblasts were isolated and cultured along with the human prostate fibroblast cell line BHPrS1in complete RPMI + 10% FBS as previously described (40, 51). Cells were plated at a density of 10,000 cells per well in a 96 well tissue culture plate, grown to around 70% confluence, serum starved in RPMI + 0.1% FBS for 24 hours, then treated with 200nM recombinant granzyme K (MyBioSource, San Diego, CA) in RPMI + 1% FBS for 24 hours (28). For senescence studies, fibroblasts were treated with 250nM doxorubicin (Sigma-Aldrich) for 24 hours, then cultured for an additional 6 days in RMPI + 10% FBS (52) prior to granzyme K treatment as described above. Supernatants were collected and analyzed for CXCL1, CCL2, CCL5, CXCL8, IL6, TNF, CCL20, IL2, and IL12p70 using the LEGENDPlex system (Biolegend) per manufacturer protocols. Comparisons with significant P values (P<0.05) are listed in Supplementary Table S1.

Statistical analyses

Statistical analyses for scRNA-Seq and bulk RNA-seq analyses are described above. For IF quantification, a two-tailed T test was

performed using GraphPad Prism (version 9; GraphPad Software, San Diego, CA). For ELISA experiments, a one-way ANOVA and Šídák's multiple comparisons test were performed using GraphPad Prism. P values less than 0.05 were considered significant.
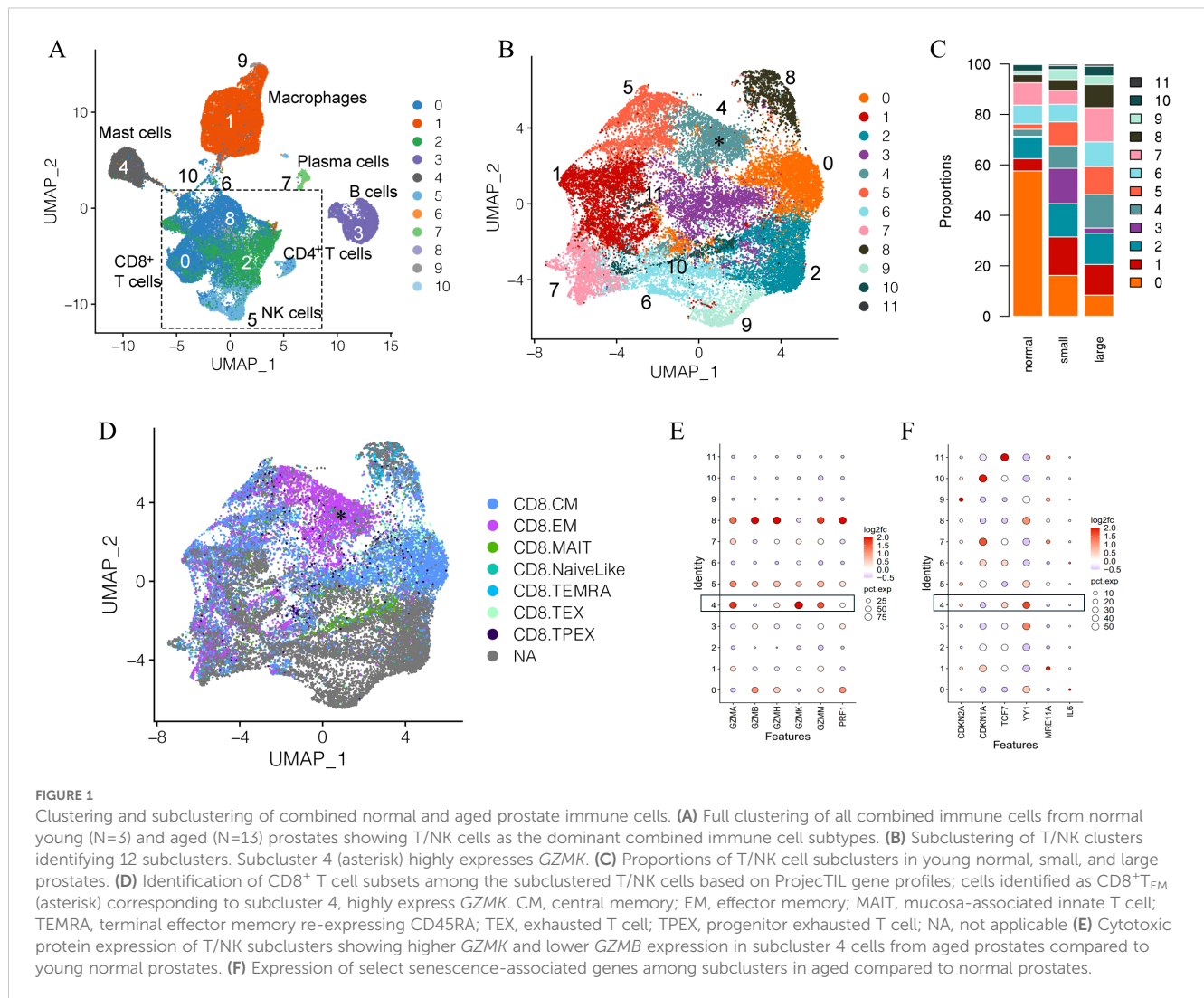
Results

A CD8+*GZMK^hi GZMB^low* Taa subset is present in aged prostates

Published scRNA-Seq data (40, 41) generated from immune cells isolated from TZ tissues collected from 10 "small" (≤40 grams) prostates and 3 "large" (≥90 grams) late-stage symptomatic prostates from aged patients were combined with immune cell scRNA-Seq data from 3 normal prostates from healthy young (age 18 to 31) organ donors with no reported comorbidities generated in a separate previously published study (42). These data were analyzed together to identify common immune cell subtypes among all samples (40, 41).

Unsupervised clustering separated immune cells into 11 clusters based on immune cell gene expression profiles (Figure 1A) (40, 41). Overall, the bulk of the combined immune cells consisted of multiple closely associated T cells and natural killer (NK) cell clusters (Figure 1A). This is generally consistent with previous studies, which identified T lymphocytes as the predominate immune cell type in the prostate (15, 34, 40, 41, 53–55). Since T cells and NK cells were the predominant immune cell type in the combined sample types, we first investigated alterations in these populations between normal and aged prostates. Cells from clusters identified as T and NK cells in the initial clustering analysis were combined and subclustered together, which separated the combined T and NK cells into 12 subclusters (Figures 1B, C, Supplementary Figures S1A, B). Subclusters were subsequently identified based on a comparison of gene expression profiles to those previously generated by ProjecTILs (Figure 1D, Supplementary Figure S1C) (56). A CD8+ subcluster identified as a central memory (T_CM) subtype (subcluster 0) made up the largest proportion of T cells in normal prostates (Figures 1B–D). While the overall number of immune cells was increased in aged prostates, the proportion of subcluster 0 T_CM cells was significantly decreased in both large and small aged prostates compared to young normal prostates (Figure 1C, Supplementary Figure S1D). A CD8+ subcluster (subcluster 4) with high expression of *GZMK* and low *GZMB* and an effector memory (T_EM)-like gene profile that was proportionally significantly increased in aged versus young normal prostates was also identified (Figures 1B–E, Supplementary Figures S1B–D) (2). These data suggest a shift in CD8+ T cell populations in aged prostates. Subcluster 4 was of particular interest due to its similar gene expression to a T cell subset previously associated with aging and referred to as Taa cells (2), prompting further investigation of this subset and its potential relationship with age-related inflammation and BPH symptoms.

In addition to a significant increase in *GZMK* expression and decrease in *GZMB* expression, the subcluster 4 Taa cells from aged prostates also showed relatively low expression of the perforin gene *PRF1* (Figure 1E). This cytotoxic protein expression pattern has

FIGURE 1

Clustering and subclustering of combined normal and aged prostate immune cells. **(A)** Full clustering of all combined immune cells from normal young (N=3) and aged (N=13) prostates showing T/NK cells as the dominant combined immune cell subtypes. **(B)** Subclustering of T/NK clusters identifying 12 subclusters. Subcluster 4 (asterisk) highly expresses *GZMK*. **(C)** Proportions of T/NK cell subclusters in young normal, small, and large prostates. **(D)** Identification of CD8$^+$ T cell subsets among the subclustered T/NK cells based on ProjecTIL gene profiles; cells identified as CD8$^+$T$_{EM}$ (asterisk) corresponding to subcluster 4, highly express *GZMK*. CM, central memory; EM, effector memory; MAIT, mucosa-associated innate T cell; TEMRA, terminal effector memory re-expressing CD45RA; TEX, exhausted T cell; TPEX, progenitor exhausted T cell; NA, not applicable **(E)** Cytotoxic protein expression of T/NK subclusters showing higher *GZMK* and lower *GZMB* expression in subcluster 4 cells from aged prostates compared to young normal prostates. **(F)** Expression of select senescence-associated genes among subclusters in aged compared to normal prostates.

been previously associated with an early-stage CD8$^+$ memory T cell differentiation state with diminished capacity for cytotoxic activity (31, 57). Expression of select cell cycle and T cell differentiation genes previously reported to be modulated in aged immune cells were differentially expressed in aged Taa cells (Figure 1F) (58–61). Expression of *YY1*, a transcription factor linked to effector T cell differentiation, autoimmunity, and senescence was significantly increased in aged prostate Taa cells (Figure 1F) (60). Expression of *CDKN2A* and *TCF7*, which encode the p16 cell cycle regulator and the T cell factor 1 (TCF1) protein associated with T cell development and maturation, respectively, were also mildly increased in aged Taa cells (Figure 1F) (58–60). Overall, these results indicate alterations in the proportion and cycle-associated gene expression profiles between Taa in young and aged prostates.

The Taa subset is positively correlated with clinical symptoms in BPH

We hypothesized that the Taa or other T cell subsets would be correlated with BPH and LUTS in aged patients. We compared

immune cell scRNA-Seq generated from aged small and large prostates (40, 41). To enhance the analysis of the Taa subset, additional immune cell scRNA-Seq data from seven large prostates were generated and integrated with the scRNA-Seq data from the thirteen aged prostates for a total of 10 small and 10 large prostate samples (40, 41).

The bulk of immune cells in the combined large and small aged prostates consisted of multiple closely associated clusters identified as T cells and NK cells (Figure 2A, Supplementary Figure S2A) (40, 41). T/NK cell subclustering analysis identified 14 subclusters (Figure 2A, Supplementary Figure S2A). Subcluster 1, identified as a CD8$^+$ T$_{EM}$-like subtype based on comparison of its gene expression profile to ProjecTILs profiles, expressed a similar high *GZMK* and low *GZMB* expression pattern as the Taa cells identified in the previous analysis (Figure 2B, Supplementary Figure S2A) (2, 56). A correlation analysis revealed that subcluster 1 Taa (R=0.7, P=0.0416) was significantly positively correlated with IPSS scores (Figure 2C) (41, 56). Additionally, a CD8$^+$ subset identified as T$_{MAIT}$ (subcluster 5) (R=0.5, P=0.0241) and a mixed T/NK cell subset (subcluster 13) (R=0.3, P=0.0282) were also positively correlated with IPSS (Figures 2B, C). Given this correlation of
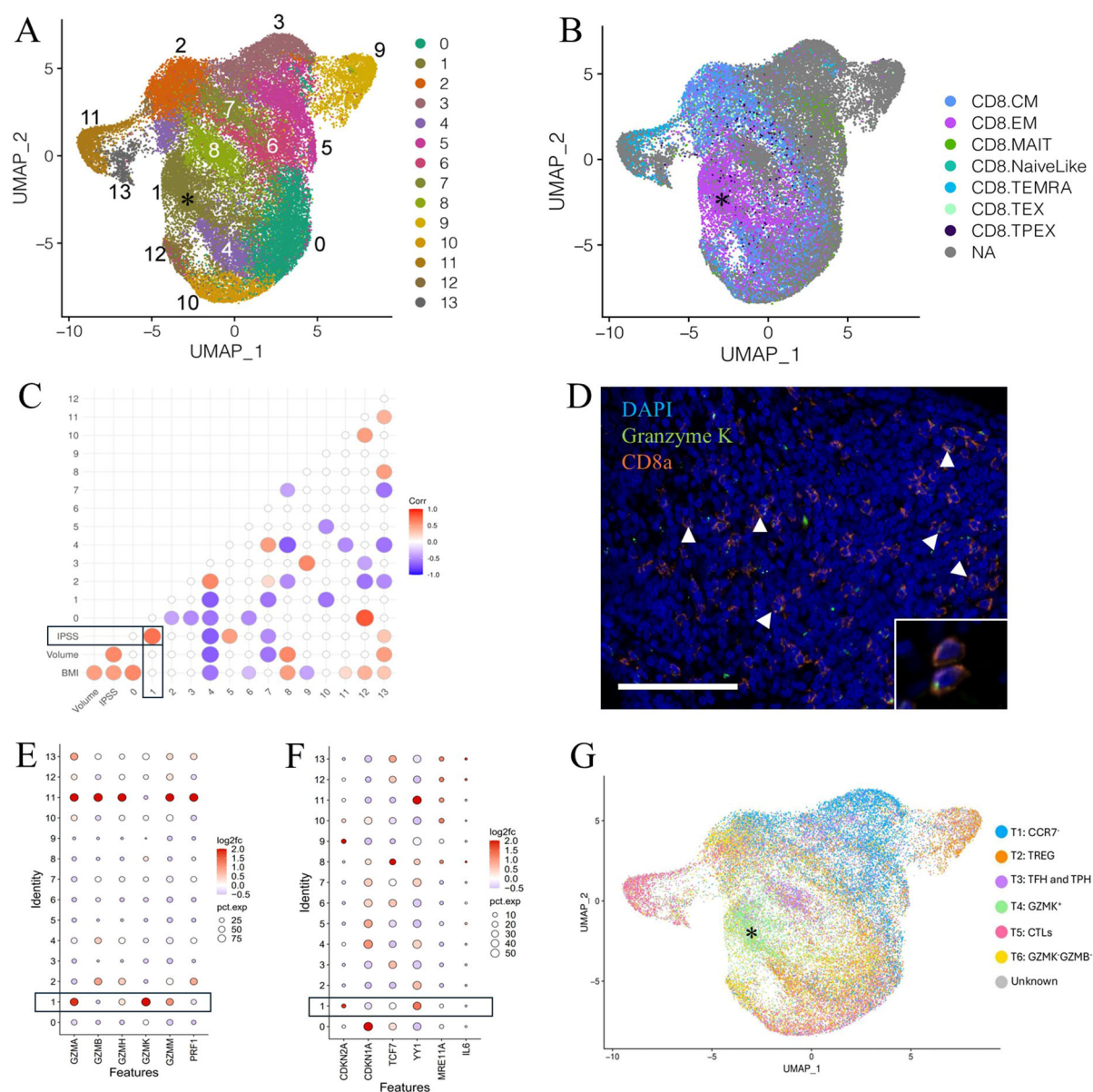
FIGURE 2

Clustering and subclustering of combined large and small aged prostate immune cells. **(A)** Figure adapted from Lanman et al. (41)[33]. Subclustering of T/NK clusters identifying 14 T/NK cell subclusters. A $GZMK^{hi}$ $GZMB^{low}$ subcluster designated Taa (asterisk) is identified. **(B)** Identification of CD8+ T cell subsets among the subclustered T/NK cells based on ProjecTILs gene profiles; subcluster 1 Taa (asterisk) with a $CD8^+$ EM-like gene expression profile, highly expresses *GZMK*. **(C)** Correlation of IPSS, prostate volume, and BMI with T/NK cell subsets; statistically significant (P<0.05) correlations are shown. **(D)** CD8a and GZMK-labeling T cells (arrowheads, inset) are identified by immunofluorescence within the prostate stromal compartment. Scale bar=100μm. **(E)** Granzyme expression of T/NK subclusters showing increased *GZMK* and decreased *GZMB* expression in subcluster 1 cells from large aged prostates compared to small aged prostates. **(F)** Expression of select senescence-associated genes among subclusters in aged compared to normal prostates. **(G)** Comparison of aged prostate and RA-derived T cells showing a common $GZMK^+$ subcluster (asterisk). TREG, regulatory T cells; TFH, Follicular helper T cells; TPH, Peripheral helper T cells; CTL, Cytotoxic T lymphocytes.

Taa with IPSS as well as previous aging studies on Taa cells, we focused our subsequent studies on Taa cells.

Lymphoid cells expressing both CD8a and GZMK were observed histologically in both small and large prostate specimens, predominately within the stroma (Figure 2D). The percentage of CD8a$^+$ cells that also labeled with GZMK was increased, albeit not significantly (P=0.0614), in large prostate tissue sections (Supplementary Figure S2B). Similarly, the

proportion of the Taa (subcluster 1) cells was not significantly increased in large prostates compared to small prostates in the scRNA-Seq analysis (Supplementary Figures S2C, D). However, there was a mild but significant increase in *GZMK* gene expression and decrease in *GZMB* gene expression as well as overall low gene expression of *PRF1* in this subcluster in large prostates compared to small (Figure 2E). Consistent with the comparison of aged and young prostate Taa cells, *YY1* and *CDKN2A* gene expression was

significantly increased in Taa cells from large prostates compared to small prostates; however, *TCF7* expression was not significantly different (Figure 2F).

Given the previous identification of *GZMK*-expressing T cells within inflamed synovial tissues of rheumatoid arthritis (RA) patients (49, 62) and the drastically increased incidence of BPH among RA patients (40, 49), we hypothesized that similar *GZMK*-expressing subsets would be present in both RA and aged prostate tissues, indicating a similar pro-inflammatory tissue microenvironment. Comparison of prostate T cell subclustering data with T cell subclustering profiles generated by Zhang et al. (49) (49) from human RA patient synovium identified 6 similar T cell subsets including a common *GZMK*-expressing subset corresponding to the Taa subcluster (Figure 2G). In all, these results support a pro-inflammatory role for *GZMK*-expressing T cells in BPH and a potential link between age-associated T cells and symptomatic BPH (49, 62). Also, the stromal location of the CD8a and GZMK-labeling cells may suggest interactions with stromal cells contribute to BPH.

T cell differentiation is shifted to the Taa subset in BPH prostates

Previous studies have described the association between CD8$^+$ memory T cell cytotoxic granules and T cell differentiation (31). *GZMK$^+$GZMB$^-$* expression has been associated with early differentiation, *GZMK$^+$GZMB$^+$* with intermediate differentiation, and *GZMK$^-$GZMB$^+$* with late-stage differentiation (31). We hypothesized that the differentiation trajectory would be altered in large prostate CD8$^+$ T cells compared to small prostates in the direction of the GZMK^{hi}GZMB^{low} Taa population. We applied a velocity analysis to the CD8$^+$ T cell subclusters to analyze the differentiation trajectories of the subclusters (45).

In both small and large prostates, overall directional flow indicated movement through CD8$^+$ T$_{CM}$ subclusters 12, 10, and 0 with most cells transitioning from T$_{CM}$ subcluster 0 towards T$_{CM}$

subcluster 7 (Figures 3A, B). In small prostates, the proportion of T$_{CM}$ subcluster 7 cells is significantly increased compared to large prostates, and most of these cells progress towards T$_{CM}$ subcluster 2 which is also significantly increased compared to large prostates (Supplementary Figure S2). T$_{CM}$ subcluster 2 expresses both *GZMB* and *PRF1* (Figure 2D), a profile associated with cytotoxicity (31). In contrast, overall movement of T cells from large prostates trended away from T$_{CM}$ subcluster 2 and towards having gene expression profiles similar to the Taa subcluster 1 (Figure 3B). Further cell cycle analyses indicated that the Taa cells were cycling with high G2M scores, particularly in large prostates, suggesting proliferation within this population (Supplementary Figures S3A, B). Overall, these results suggest altered directional flow and differentiation of the CD8$^+$ T cell subclusters between large and small specimens. This altered differentiation may contribute to the overall change in T cell subcluster proportions between small and large prostates through diversion of trajectory from a *GZMB* and *PRF1*-expressing cytotoxic population (T$_{CM}$ subcluster 7) towards the proliferating Taa as a terminal phenotype in large prostates. Notably, subcluster 7 is also statistically significantly negatively correlated (R=-0.5, P=0.0294) with IPSS (Figure 2C), further suggesting that this shifted trajectory contributes to LUTS.

SASP and senescence-associated genes are expressed by BPH stromal cells

We hypothesized that SASP-associated cytokine gene expression might correlate with prostatic cellular expansion. We used bulk RNA-Seq data from small and large aged prostates used in the scRNA-Seq analyses to examine the overall SASP-associated cytokine expression in whole prostate specimens. SASP cytokine expression varied among the specimens and was not consistent among the small or large prostate groups (Figure 4A). We then examined SASP gene expression in specific prostate cellular populations using combined all-cell scRNA-Seq data generated from 5 large BPH prostates (40). As the Taa cells were located predominantly within the stromal
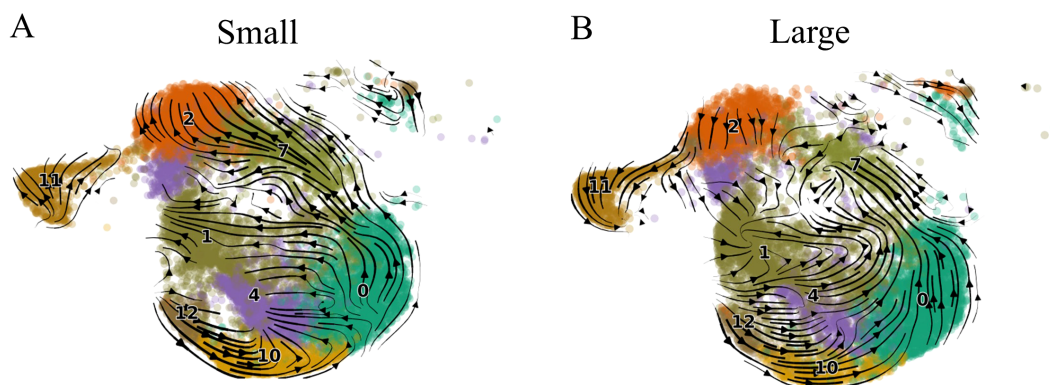

FIGURE 3
Velocity analysis of small and large aged prostate CD8$^+$ T cell subsets. **(A)** Velocity results for small prostate CD8$^+$ T cells. **(B)** Velocity results for large prostate CD8$^+$ T cells. Arrows indicate directional flow of cells in the low-dimensional embedding (UMAP), the direction of which essentially denotes the predicted differentiation trajectory of the cells.
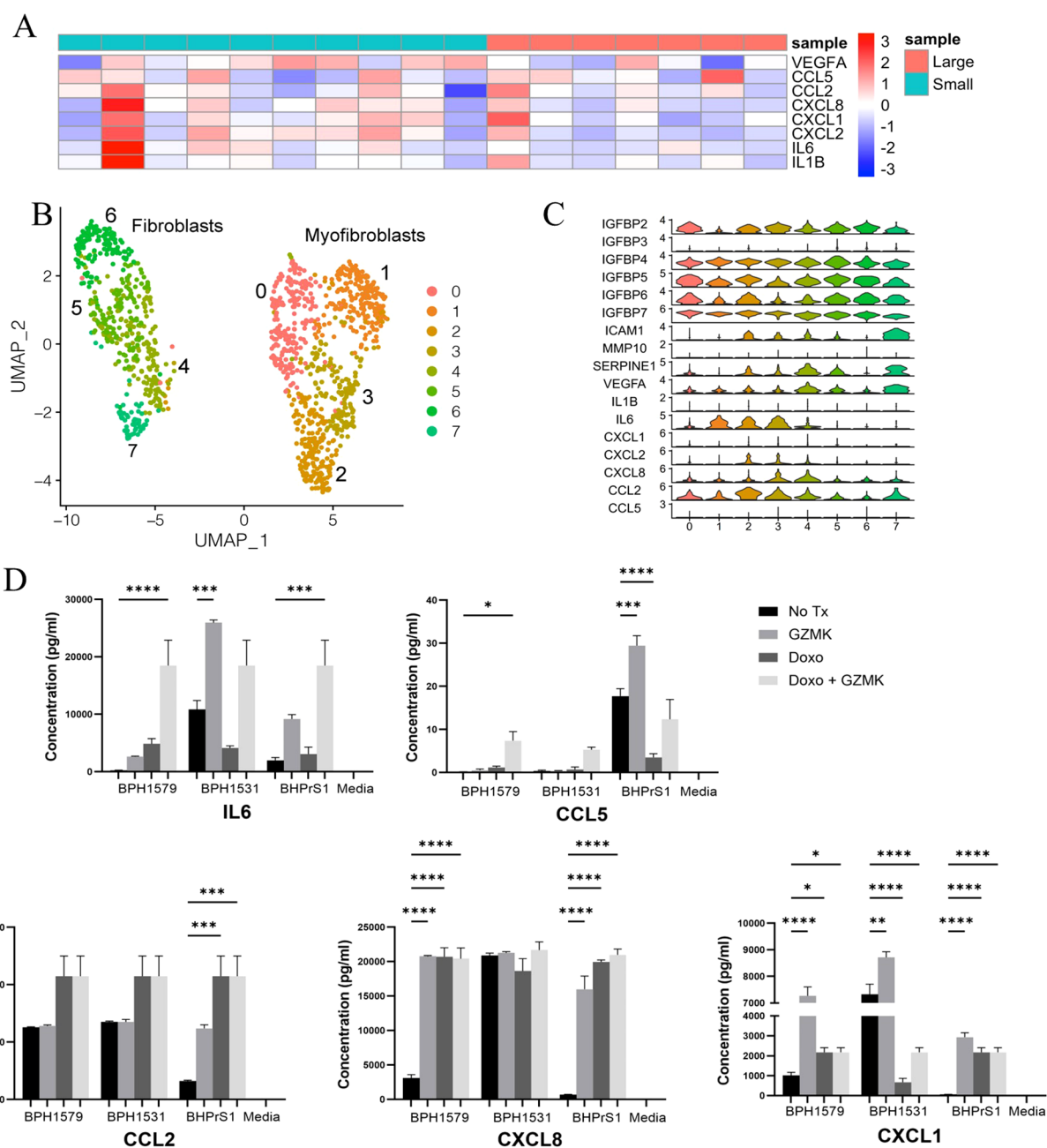
FIGURE 4

SASP-associated cytokine and chemokine expression in BPH prostates **(A)** Cytokine Heatmap. Log₂(FPKM) values of cytokine genes in bulk RNA-seq data from large and small prostate specimens is shown in a heatmap, with row scaling performed. The color of the annotation bar above columns indicates sample identity (Large vs Small) and the color of the rows indicates gene expression from high (red) to low (blue). **(B)** Subclustering of stromal cells from 5 large aged prostates **(C)** SASP-associated gene expression among stromal cell subclusters. **(D)** Production of SASP-associated cytokines with at least one statistically significantly (P<0.05)modulated specimen following in vitro granzyme K treatment of cycling and Doxorubicin (Doxo)-treated senescent BPH patient-derived fibroblasts. Adjusted P values for all comparisons are listed in Supplementary Table S1. * = P value 0.01 to 0.05, ** = P value 0.001 to 0,1, *** = P value 0.0001 to 0.001, **** = P value < 0.0001.

compartment histologically (Supplementary Figure S4A), and that granzyme K has been shown to induce SASP in stromal cells in other organs (2, 28), we hypothesized that Taa cells might impact SASP production by stromal cells and contribute to a proinflammatory microenvironment (2, 28). We subclustered the stromal cells and identified genes associated with SASP and senescence, and particularly expression of SASP-associated cytokine genes

reportedly induced by granzyme K (2, 28). We also subclustered T cells to determine whether the Taa subcluster identified in the immune cell analyses could be identified in the all-cell analysis. Stromal cell subclustering identified 8 subclusters segregated into two groupings of 4 subclusters, with one grouping identified as smooth muscle cell/myofibroblasts and the other as fibroblasts based on DEGs (Figure 4B). Expression of SASP-associated genes

among stromal cell subclusters showed variable expression among the subclusters, including genes for GZMK-induced cytokines *CXCL8, CXCL1, IL6, CCL2,* and *CXCL2* (Figure 4C) (2, 28). Additionally, a *GZMK*hi *GZMB*low Taa subcluster was identified among T cells (Supplementary Figures S4A, B). These results indicate SASP-associated pro-inflammatory cytokine gene expression by prostate stromal cells.

Granzyme K modulates SASP-associated cytokine production by cycling and senescent BPH fibroblasts *in vitro*

Since scRNA-seq data showed senescence-associated and SASP-associated cytokine/chemokine gene expression in prostate stromal cells, we hypothesized that granzyme K secreted by Taa may modulate senescence-associated gene expression in fibroblasts and stimulate BPH fibroblasts to produce SASP-associated cytokines/chemokines. To assess the potential impact of granzyme K on prostate stromal cells, BPH patient-derived fibroblast cell line BHPrS1 and primary fibroblasts derived from two BPH patients (51) were treated with granzyme K *in vitro*. Doxorubicin (Doxo) treatment to induce senescence (52) was included to observe whether granzyme K stimulation can further promote SASP in senescent fibroblasts. In both cycling and Doxo-treated senescent fibroblasts, *in vitro* granzyme K treatment significantly increased ($P<0.05$) secretion of one or more SASP-associated cytokines IL-6, CXCL8, CCL5, CCL2, and CXCL1 in at least one prostate fibroblast specimen (Figure 4D, Supplementary Table S1), and this effect varied among the fibroblast specimens. Overall, these data show that granzyme K can modulate SASP-associated factor secretion by BPH-derived fibroblasts and suggests that granzyme K may impact the prostate inflammatory microenvironment by promoting inflammatory cytokine production by both cycling and senescent prostate stromal fibroblasts. Additionally, the variability in granzyme K-induced cytokine production among the BPH patient-derived fibroblasts is compatible with the clinical and morphologic variability observed among BPH patients.

Discussion

In this study, we identified a CD8+*GZMK*hi*GZMB*low Taa subset previously associated with aging present within the stromal compartment and correlated with IPSS in aged prostates (2). Consistent with involvement in other inflammatory diseases, prostate Taa cells shared a similar gene expression profile to a *GZMK*-expressing RA T cell subset, further suggesting a potential role for granzyme K-expressing cells in promoting a dysregulated and pro-inflammatory immune microenvironment (49, 62). *In vitro* granzyme K treatment of prostate fibroblasts indicates granzyme K can stimulate pro-inflammatory cytokine and chemokine production by prostate stromal cells. While a specific function for Taa cells has not yet been defined (2), these data suggest that Taa may contribute to BPH-associated inflammation and IPSS through

granzyme K-mediated stimulation of stromal cell cytokine and chemokine production leading to recruitment and activation of additional immune cells in the prostate microenvironment.

Of the five granzymes (A, B, H, K, M) identified in humans, granzyme K is the least well studied (63). While the functions of granzyme K are currently not well defined, previous studies have identified intracellular and extracellular roles for granzyme K which include both cytotoxic and non-cytotoxic activities (63, 64). However, unlike the most common cytotoxic granzyme GZMB, which in combination with perforin (PRF1) is associated with induction of apoptotic cell death, GZMK lacks lytic activity and its expression has not been positively correlated with cytotoxic activity (31, 63). Also, unlike other granzymes, a cellular receptor for GZMK has not been identified. In addition to low *GZMB* and high *GZMK* gene expression, Taa cells showed low *PRF1* expression, further suggesting reduced cytotoxic capacity in these cells (Figures 1F, 2C). T cell cytotoxic capacity and ability to eliminate infected or neoplastic cells diminishes with age, suggesting an association between an increased proportion of *GZMK*hi T cells and diminished cytotoxic activity with aging (31). Additionally, expression of *YY1*, a gene that has been associated with both cellular senescence and T cell-mediated diseases, and *CDKN2A*, a gene involved in senescence-associated cell cycle arrest, were increased in large prostate Taa cells, further suggesting alterations in this T cell population between small and large prostates (58–60).

As T cell differentiation involves the maturation of lytic granules, we hypothesized that the changes in granzyme gene expression may indicate altered T cell differentiation between large and small aged prostates (31, 32). RNA velocity analysis was used to infer the differentiation fates of CD8+ T cell subsets (45, 65, 66). A high proportion of unspliced transcripts for a particular gene indicates upregulation of that gene, and RNA velocity analysis describes changes in the abundance of mRNA transcripts (45). By examining the velocities of multiple genes, the differentiation pathways of individual cells may be inferred (45). Genes were ranked on velocity to find genes in a subcluster that show dynamics that are transcriptionally differently regulated compared to all other subclusters, for example, induction in that cluster and homeostasis in the remaining population. In the current study, directional flow to and from the Taa population is altered between large and small aged prostates (31). Also, evidence of cycling in the Taa subcluster suggests these cells are proliferating, which may also contribute to the accumulation of these cells in large prostates.

Conclusions

In this study, we identified a previously described GZMK-high Taa subset in aged prostates that was correlated with IPSS. Expression of granzyme and senescence-associated genes was altered in this subset between normal and aged and between small and large aged prostates. Velocity analyses suggested that altered T cell differentiation trajectory may contribute to accumulation of Taa cells in large vs small aged prostates. Aged

prostate fibroblasts express multiple SASP-associated genes, and GZMK variably induces SASP-associated cytokine expression in prostate fibroblasts *in vitro*, suggesting that Taa cells may promote prostate cellular expansion and immune cell recruitment through GZMK-induced fibroblast SASP production. Variability in SASP gene expression among small and large aged prostates and variable responses of BPH patient-derived fibroblasts to GZMK *in vitro* are compatible with the variability in symptoms and response to treatment observed clinically among BPH patients and highlights that BPH is likely multifactorial involving multiple cellular processes that have yet to be fully defined. Overall, the findings of the current study suggest a potential role for the age-associated Taa in BPH.

Future directions

It is hypothesized that the interplay of Taa cells and stromal cells may contribute to the non-resolving and progressive inflammation of BPH though granzyme K-mediated SASP cytokines and chemokines. A similar effect has been described in concurrent studies involving myeloid cells (41). However, while the secretion of multiple SASP cytokines and chemokines were modulated by prostate fibroblast granzyme K treatment *in vitro*, further studies are needed to confirm a direct fibroblast stimulatory capacity for Taa cells and if Taa cells have a causal role in the development and progression of BPH-associated inflammation and LUTS. Additionally, further study is needed to determine the underlying mechanisms for altered T cell differentiation and gene expression and to define the clinical consequences of these alterations. For example, in addition to SASP genes, stromal cell subclusters expressed *CDKN1A*, *YY1*, and *IL6*, genes that have been previously linked to cellular senescence (Supplementary Figure S4C) (67). Also, YY1, which has been shown to repress p16 expression and curtail senescence in cancer cells, has also been associated with collagen production and implicated in fibrotic diseases such as idiopathic pulmonary fibrosis (IPF) and liver fibrosis through promoting myofibroblasts differentiation and increased collagen production by fibroblasts and myofibroblasts (68–71). As other studies have suggested a role for prostatic fibrosis in contributing to BPH-associated LUTS, these results may indicate a role for YY1 signaling in BPH (72). More recently, a role for granzyme K-mediated complement activation in RA and other chronic inflammatory conditions has been described (73). Complement has been shown to be highly expressed by synovial fibroblasts and promote fibroblast-mediated inflammatory tissue priming in RA (74) and has been explored as a potential therapeutic target and biomarker for RA (75, 76). Given the similarities between BPH and RA inflammation, granzyme K-mediated complement activation and fibroblast stimulation may play a role in driving BPH inflammation and LUTS. In all, this warrants further investigation of Taa cells as a potential therapeutic target or biomarker for management of BPH inflammation, fibrosis, and LUTS.

While the current study focused on CD8$^+$ T cells and specifically Taa cells, other T cell subsets were positively correlated with IPSS and/or prostate volume (Figure 2C). This includes a CD8$^+$ T$_{MAIT}$ subset, and CD8$^+$ T$_{MAIT}$ cells have previously been implicated in immune-mediated inflammatory diseases (77, 78). Future studies of the role of aging and T cells in BPH include investigating this and other specific T cell subsets, as well as epigenetic alterations or changes in T cell receptor (TCR) repertoires with age, and exploring interactions between stromal and epithelial cells with immune cells (11, 79, 80). Furthermore, the impact of androgens on aging prostate immune cells is yet to be explored, particularly in the context of androgen-targeted therapy for BPH. While most BPH patients initially respond to androgen-targeted therapy, many eventually progress and require surgical intervention for their LUTS (81). Further studies in this area may elucidate the roles of age-associated alterations in androgens and immunity in treatment failure. These current and future studies could benefit BPH patients by providing potential immunological biomarkers or pharmaceutical targets for improved prognostics and medical management of BPH and LUTS.

Limitations of the study

Several challenges were encountered in this study. As surgical intervention is not indicated for patients without bothersome urinary symptoms or without evidence of PCa, therefore small, aged prostates were collected from PCa patients with small PZ-confined tumors (40, 41). The field effects of PCa tumors are considered limited to within about 3mm of the tumor periphery (82, 83). For these reasons, PCa-free TZ tissue obtained from these specimens is an accepted method for collection of these samples (82, 83). However, the potential effects of PZ tumor cells on TZ immune cells cannot be completely ruled out. Another challenge in this study was related to the previously published normal non-BPH prostate scRNA-Seq study by Henry et al. (42), which all prostate cells rather than isolated CD45$^+$ leukocytes were analyzed (42). The inclusion of more numerous prostate cell populations along with the relatively small number of immune cells normally present in non-BPH prostates meant there were relatively few normal prostate immune cells for analysis compared to our BPH specimens. Consequently, this may have affected some analyses and prevented the inclusion of normal immune cells in some analyses.

Data availability statement

The datasets presented in this study can be found in online repositories. The names of the repository/repositories and accession number(s) can be found below: https://www.ncbi.nlm.nih.gov/geo/, GSE120716 https://www.ncbi.nlm.nih.gov/geo/, GSE269205 https://www.ncbi.nlm.nih.gov/geo/, GSE183676.

Ethics statement

The studies involving humans were approved by NorthShore University HealthSystem Institutional Review Board, Endeavor

Health, Evanston IL. The studies were conducted in accordance with the local legislation and institutional requirements. The human samples used in this study were acquired from primarily isolated as part of your previous study for which ethical approval was obtained. Written informed consent for participation was not required from the participants or the participants' legal guardians/next of kin in accordance with the national legislation and institutional requirements.

Conflict of interest

The authors declare that the research was conducted in the absence of any commercial or financial relationships that could be construed as a potential conflict of interest.

Generative AI statement

The author(s) declare that no Generative AI was used in the creation of this manuscript.

Publisher's note

All claims expressed in this article are solely those of the authors and do not necessarily represent those of their affiliated organizations, or those of the publisher, the editors and the reviewers. Any product that may be evaluated in this article, or claim that may be made by its manufacturer, is not guaranteed or endorsed by the publisher.

Supplementary material

The Supplementary Material for this article can be found online at: https://www.frontiersin.org/articles/10.3389/fimmu.2025.1585446/full#supplementary-material

References

1. Franceschi C, Garagnani P, Parini P, Giuliani C, Santoro A. Inflammaging: a new immune-metabolic viewpoint for age-related diseases. *Nat Rev Endocrinol*. (2018) 14:576–90. doi: 10.1038/s41574-018-0059-4

2. Mogilenko DA, Shpynov O, Andhey PS, Arthur L, Swain A, Esaulova E, et al. Comprehensive profiling of an aging immune system reveals clonal GZMK(+) CD8(+) T cells as conserved hallmark of inflammaging. *Immunity*. (2021) 54:99–115 e12. doi: 10.1016/j.immuni.2020.11.005

3. Zhou D, Borsa M, Simon AK. Hallmarks and detection techniques of cellular senescence and cellular ageing in immune cells. *Aging Cell*. (2021) 20:e13316. doi: 10.1111/acel.13316

4. Pangrazzi L, Weinberger B. T cells, aging and senescence. *Exp Gerontol*. (2020) 134:110887. doi: 10.1016/j.exger.2020.110887

5. Montecino-Rodriguez E, Berent-Maoz B, Dorshkind K. Causes, consequences, and reversal of immune system aging. *J Clin Invest*. (2013) 123:958–65. doi: 10.1172/JCI64096

6. Mogilenko DA, Shchukina I, Artyomov MN. Immune ageing at single-cell resolution. *Nat Rev Immunol*. (2021) 22(8):484–498. doi: 10.1038/s41577-021-00646-4

7. Lopez-Otin C, Blasco MA, Partridge L, Serrano M, Kroemer G. The hallmarks of aging. *Cell*. (2013) 153:1194–217. doi: 10.1016/j.cell.2013.05.039

8. Aw D, Silva AB, Palmer DB. Immunosenescence: emerging challenges for an ageing population. *Immunology*. (2007) 120:435–46. doi: 10.1111/j.1365-2567.2007.02555.x

9. Rodriguez IJ, Lalinde Ruiz N, Llano Leon M, Martinez Enriquez L, Montilla Velasquez MDP, Ortiz Aguirre JP, et al. Immunosenescence study of T cells: A systematic review. *Front Immunol*. (2020) 11:604591. doi: 10.3389/fimmu.2020.604591

10. Fulop T, Dupuis G, Witkowski JM, Larbi A. The role of immunosenescence in the development of age-related diseases. *Rev Invest Clin*. (2016) 68:84–91.

11. Masters AR, Haynes L, Su DM, Palmer DB. Immune senescence: significance of the stromal microenvironment. *Clin Exp Immunol*. (2017) 187:6–15. doi: 10.1111/cei.12851

12. Campisi J, Kapahi P, Lithgow GJ, Melov S, Newman JC, Verdin E. From discoveries in ageing research to therapeutics for healthy ageing. *Nature*. (2019) 571:183–92. doi: 10.1038/s41586-019-1365-2

13. Da Silva PFL, Ogrodnik M, Kucheryavenko O, Glibert J, Miwa S, Cameron K, et al. The bystander effect contributes to the accumulation of senescent cells in *vivo*. *Aging Cell*. (2019) 18:e12848. doi: 10.1111/acel.2019.18.issue-1

14. Berry SJ, Coffey DS, Walsh PC, Ewing LL. The development of human benign prostatic hyperplasia with age. *J Urol*. (1984) 132:474–9. doi: 10.1016/S0022-5347(17)49698-4

15. Robert G, Descazeaud A, Nicolaiew N, Terry S, Sirab N, Vacherot F, et al. Inflammation in benign prostatic hyperplasia: a 282 patients' immunohistochemical analysis. *Prostate*. (2009) 69:1774–80. doi: 10.1002/pros.v69:16

16. Vital P, Castro P, Ittmann M. Oxidative stress promotes benign prostatic hyperplasia. *Prostate*. (2016) 76:58–67. doi: 10.1002/pros.23100

17. Franks LM. Benign nodular hyperplasia of the prostate; a review. *Ann R Coll Surg Engl*. (1953) 14:92–106.

18. Bierhoff E, Vogel J, Benz M, Giefer T, Wernert N, Pfeifer U. Stromal nodules in benign prostatic hyperplasia. *Eur Urol*. (1996) 29:345–54. doi: 10.1159/000473774

19. Nickel JC, Downey J, Young I, Boag S. Asymptomatic inflammation and/or infection in benign prostatic hyperplasia. *BJU Int*. (1999) 84:976–81. doi: 10.1046/j.1464-410x.1999.00352.x

20. Choi J, Shendrik I, Peacocke M, Peehl D, Buttyan R, Ikeguchi EF, et al. Expression of senescence-associated beta-galactosidase in enlarged prostates from men with benign prostatic hyperplasia. *Urology*. (2000) 56:160–6. doi: 10.1016/S0090-4295(00)00538-0

21. Jiang S, Song CS, Chatterjee B. Stimulation of prostate cells by the senescence phenotype of epithelial and stromal cells: implication for benign prostate hyperplasia. *FASEB Bioadv*. (2019) 1:353–63. doi: 10.1096/fba.2018-00084

22. Vignozzi L, Rastrelli G, Corona G, Gacci M, Forti G, Maggi M. Benign prostatic hyperplasia: a new metabolic disease? *J Endocrinol Invest*. (2014) 37:313–22. doi: 10.1007/s40618-014-0051-3

23. Nickel JC, Roehrborn CG, Castro-Santamaria R, Freedland SJ, Moreira DM. Chronic prostate inflammation is associated with severity and progression of benign prostatic hyperplasia, lower urinary tract symptoms and risk of acute urinary retention. *J Urol*. (2016) 196:1493–8. doi: 10.1016/j.juro.2016.06.090

24. Sauver JLS, Jacobson DJ, Mcgree ME, Girman CJ, Lieber MM, Jacobsen SJ. Longitudinal association between prostatitis and development of benign prostatic hyperplasia. *Urology*. (2008) 71:475–9. doi: 10.1016/j.urology.2007.11.155

25. Ou Z, He Y, Qi L, Zu X, Wu L, Cao Z, et al. Infiltrating mast cells enhance benign prostatic hyperplasia through IL-6/STAT3/Cyclin D1 signals. *Oncotarget*. (2017) 8:59156–64. doi: 10.18632/oncotarget.19465

26. Kramer G, Steiner GE, Handisurya A, Stix U, Haitel A, Knerer B, et al. Increased expression of lymphocyte-derived cytokines in benign hyperplastic prostate tissue, identification of the producing cell types, and effect of differentially expressed cytokines on stromal cell proliferation. *Prostate*. (2002) 52:43–58. doi: 10.1002/pros.10084

27. Begley LA, Kasina S, Macdonald J, Macoska JA. The inflammatory microenvironment of the aging prostate facilitates cellular proliferation and hypertrophy. *Cytokine*. (2008) 43:194–9. doi: 10.1016/j.cyto.2008.05.012

28. Cooper DM, Pechkovsky DV, Hackett TL, Knight DA, Granville DJ. Granzyme K activates protease-activated receptor-1. *PloS One*. (2011) 6:e21484. doi: 10.1371/journal.pone.0021484

29. Wensink AC, Hack CE, Bovenschen N. Granzymes regulate proinflammatory cytokine responses. *J Immunol*. (2015) 194:491–7. doi: 10.1007/s40618-014-0051-3

30. Kaiserman D, Zhao P, Rowe CL, Leong A, Barlow N, Joeckel LT, et al. Granzyme K initiates IL-6 and IL-8 release from epithelial cells by activating protease-activated receptor 2. *PloS One*. (2022) 17:e0270584. doi: 10.1371/journal.pone.0270584

31. Harari A, Bellutti Enders F, Cellerai C, Bart PA, Pantaleo G. Distinct profiles of cytotoxic granules in memory CD8 T cells correlate with function, differentiation stage, and antigen exposure. *J Virol*. (2009) 83:2862–71. doi: 10.1128/JVI.02528-08

32. Sanchez-Ruiz Y, Valitutti S, Dupre L. Stepwise maturation of lytic granules during differentiation and activation of human CD8+ T lymphocytes. *PloS One*. (2011) 6:e27057. doi: 10.1371/journal.pone.0027057

33. Kramer G, Marberger M. Could inflammation be a key component in the progression of benign prostatic hyperplasia? *Curr Opin Urol*. (2006) 16:25–9. doi: 10.1097/01.mou.0000193368.91823.1b

34. Kramer G, Mitteregger D, Marberger M. Is benign prostatic hyperplasia (BPH) an immune inflammatory disease? *Eur Urol*. (2007) 51:1202–16. doi: 10.1016/j.eururo.2006.12.011

35. Moore RA. Inflammation of the prostate gland. *J Urol*. (1937) 38:173–81. doi: 10.1016/S0022-5347(17)71941-6

36. De Nunzio C, Aronson W, Freedland SJ, Giovannucci E, Parsons JK. The correlation between metabolic syndrome and prostatic diseases. *Eur Urol*. (2012) 61:560–70. doi: 10.1016/j.eururo.2011.11.013

37. Parsons JK, Carter HB, Partin AW, Windham BG, Metter EJ, Ferrucci L, et al. Metabolic factors associated with benign prostatic hyperplasia. *J Clin Endocrinol Metab*. (2006) 91:2562–8. doi: 10.1210/jc.2005-2799

38. Gacci M, Corona G, Vignozzi L, Salvi M, Serni S, De Nunzio C, et al. Metabolic syndrome and benign prostatic enlargement: a systematic review and meta-analysis. *BJU Int*. (2015) 115:24–31. doi: 10.1111/bju.12728

39. Zhao TV, Sato Y, Goronzy JJ, Weyand CM. T-cell aging-associated phenotypes in autoimmune disease. *Front Aging*. (2022) 3:867950. doi: 10.3389/fragi.2022.867950

40. Vickman RE, Aaron-Brooks L, Zhang R, Lanman NA, Lapin B, Gil V, et al. TNF is a potential therapeutic target to suppress prostatic inflammation and hyperplasia in autoimmune disease. *Nat Commun*. (2022) 13:2133. doi: 10.1038/s41467-022-29719-1

41. Lanman NA, Meco E, Fitchev P, Kolliegbo AK, Broman MM, Filipovich Y, et al. Infiltrating lipid-rich macrophage subpopulations identified as a regulator of increasing prostate size in human benign prostatic hyperplasia. *Front Immunol*. (2024) 15:1494476. doi: 10.3389/fimmu.2024.1494476

42. Henry GH, Malewska A, Joseph DB, Malladi VS, Lee J, Torrealba J, et al. A cellular anatomy of the normal adult human prostate and prostatic urethra. *Cell Rep*. (2018) 25:3530–3542 e5. doi: 10.1016/j.celrep.2018.11.086

43. La Manno G, Soldatov R, Zeisel A, Braun E, Hochgerner H, Petukhov V, et al. RNA velocity of single cells. *Nature*. (2018) 560:494–8. doi: 10.1038/s41586-018-0414-6

44. Stuart T, Butler A, Hoffman P, Hafemeister C, Papalexi E, Mauck WM, et al. Comprehensive integration of single-cell data. *Cell*. (2019) 177:1888–1902 e21. doi: 10.1016/j.cell.2019.05.031

45. Bergen V, Lange M, Peidli S, Wolf FA, Theis FJ. Generalizing RNA velocity to transient cell states through dynamical modeling. *Nat Biotechnol*. (2020) 38:1408–14. doi: 10.1038/s41587-020-0591-3

46. Dobin A, Davis CA, Schlesinger F, Drenkow J, Zaleski C, Jha S, et al. STAR: ultrafast universal RNA-seq aligner. *Bioinformatics*. (2013) 29:15–21. doi: 10.1093/bioinformatics/bts635

47. Liao Y, Smyth GK, Shi W. featureCounts: an efficient general purpose program for assigning sequence reads to genomic features. *Bioinformatics*. (2014) 30:923–30. doi: 10.1093/bioinformatics/btt656

48. Anders S, Huber W. Differential expression analysis for sequence count data. *Genome Biol*. (2010) 11:R106. doi: 10.1186/gb-2010-11-10-r106

49. Zhang F, Wei K, Slowikowski K, Fonseka CY, Rao DA, Kelly S, et al. Defining inflammatory cell states in rheumatoid arthritis joint synovial tissues by integrating single-cell transcriptomics and mass cytometry. *Nat Immunol*. (2019) 20:928–42. doi: 10.1038/s41590-019-0378-1

50. Pliner HA, Shendure J, Trapnell C. Supervised classification enables rapid annotation of cell atlases. *Nat Methods*. (2019) 16:983–6. doi: 10.1038/s41592-019-0535-3

51. Franco OE, Jiang M, Strand DW, Peacock J, Fernandez S, Jackson RS, et al. Altered TGF-beta signaling in a subpopulation of human stromal cells promotes prostatic carcinogenesis. *Cancer Res*. (2011) 71:1272–81. doi: 10.1158/0008-5472.CAN-10-3142

52. Hernandez-Segura A, Brandenburg S, Demaria M. Induction and validation of cellular senescence in primary human cells. *J Vis Exp*. (2018) 136:57782. doi: 10.3791/57782

53. Theyer G, Kramer G, Assmann I, Sherwood E, Preinfalk W, Marberger M, et al. Phenotypic characterization of infiltrating leukocytes in benign prostatic hyperplasia. *Lab Invest*. (1992) 66:96–107.

54. Di Carlo E, Magnasco S, D'antuono T, Tenaglia R, Sorrentino C. The prostate-associated lymphoid tissue (PALT) is linked to the expression of homing chemokines CXCL13 and CCL21. *Prostate*. (2007) 67:1070–80. doi: 10.1002/pros.20604

55. Tuong ZK, Loudon KW, Berry B, Richoz N, Jones J, Tan X, et al. Resolving the immune landscape of human prostate at a single-cell level in health and cancer. *Cell Rep*. (2021) 37:110132. doi: 10.1016/j.celrep.2021.110132

56. Andreatta M, Corria-Osorio J, Muller S, Cubas R, Coukos G, Carmona SJ. Interpretation of T cell states from single-cell transcriptomics data using reference atlases. *Nat Commun*. (2021) 12:2965. doi: 10.1038/s41467-021-23324-4

57. Bratke K, Kuepper M, Bade B, Virchow JC Jr., Luttmann W. Differential expression of human granzymes A, B, and K in natural killer cells and during CD8+ T cell differentiation in peripheral blood. *Eur J Immunol*. (2005) 35:2608–16. doi: 10.1002/eji.200526122

58. Safwan-Zaiter H, Wagner N, Michiels JF, Wagner KD. Dynamic spatiotemporal expression pattern of the senescence-associated factor p16Ink4a in development and aging. *Cells*. (2022) 11:541. doi: 10.3390/cells11030541

59. Safwan-Zaiter H, Wagner N, Wagner KD. P16INK4A-more than a senescence marker. *Life (Basel)*. (2022) 12(9):1332. doi: 10.3390/life12091332

60. Kosasih FR, Bonavida B. Involvement of yin yang 1 (YY1) expression in T-cell subsets differentiation and their functions: implications in T cell-mediated diseases. *Crit Rev Immunol*. (2019) 39:491–510. doi: 10.1615/CritRevImmunol.2020033272

61. Kim C, Jin J, Weyand CM, Goronzy JJ. The transcription factor TCF1 in T cell differentiation and aging. *Int J Mol Sci*. (2020) 21(18):6497. doi: 10.3390/ijms21186497

62. Jonsson AH, Zhang F, Dunlap G, Gomez-Rivas E, Watts GFM, Faust HJ, et al. Granzyme K(+) CD8 T cells form a core population in inflamed human tissue. *Sci Transl Med*. (2022) 14:eabo0686. doi: 10.1126/scitranslmed.abo0686

63. Bouwman AC, Van Daalen KR, Crnko S, Ten Broeke T, Bovenschen N. Intracellular and extracellular roles of granzyme K. *Front Immunol*. (2021) 12:677707. doi: 10.3389/fimmu.2021.677707

64. Anthony DA, Andrews DM, Watt SV, Trapani JA, Smyth MJ. Functional dissection of the granzyme family: cell death and inflammation. *Immunol Rev*. (2010) 235:73–92. doi: 10.1111/j.0105-2896.2010.00907.x

65. Griffiths JA, Scialdone A, Marioni JC. Using single-cell genomics to understand developmental processes and cell fate decisions. *Mol Syst Biol*. (2018) 14:e8046. doi: 10.15252/msb.20178046

66. Kulkarni A, Anderson AG, Merullo DP, Konopka G. Beyond bulk: a review of single cell transcriptomics methodologies and applications. *Curr Opin Biotechnol*. (2019) 58:129–36. doi: 10.1016/j.copbio.2019.03.001

67. Perucca P, Cazzalini O, Madine M, Savio M, Laskey RA, Vannini V, et al. Loss of p21 CDKN1A impairs entry to quiescence and activates a DNA damage response in normal fibroblasts induced to quiescence. *Cell Cycle*. (2009) 8:105–14. doi: 10.4161/cc.8.1.7507

68. Lin X, Sime PJ, Xu H, Williams MA, Larussa L, Georas SN, et al. Yin yang 1 is a novel regulator of pulmonary fibrosis. *Am J Respir Crit Care Med*. (2011) 183:1689–97. doi: 10.1164/rccm.201002-0232OC

69. Wang X, Feng Y, Xu L, Chen Y, Zhang Y, Su D, et al. YY1 restrained cell senescence through repressing the transcription of p16. *Biochim Biophys Acta*. (2008) 1783:1876–83. doi: 10.1016/j.bbamcr.2008.05.015

70. Liu H, Zhang S, Xu S, Koroleva M, Small EM, Jin ZG. Myofibroblast-specific YY1 promotes liver fibrosis. *Biochem Biophys Res Commun*. (2019) 514:913–8. doi: 10.1016/j.bbrc.2019.05.004

71. Riquet FB, Tan L, Choy BK, Osaki M, Karsenty G, Osborne TF, et al. YY1 is a positive regulator of transcription of the Col1a1 gene. *J Biol Chem*. (2001) 276:38665–72. doi: 10.1074/jbc.M009881200

72. Bushman WA, Jerde TJ. The role of prostate inflammation and fibrosis in lower urinary tract symptoms. *Am J Physiol Renal Physiol*. (2016) 311:F817–21. doi: 10.1152/ajprenal.00602.2015

73. Donado CA, Jonsson AH, Theisen E, Zhang F, Nathan A, Rupani KV, et al. Granzyme K drives a newly-intentified pathway of complement activation. *Nature*. (2024) 641:211–21. doi: 10.1101/2024.05.22.595315

74. Friscic J, Bottcher M, Reinwald C, Bruns H, Wirth B, Popp SJ, et al. The complement system drives local inflammatory tissue priming by metabolic reprogramming of synovial fibroblasts. *Immunity*. (2021) 54:1002–1021 e10. doi: 10.1016/j.immuni.2021.03.003

75. Nguyen THP, Hokstad I, Fagerland MW, Mollnes TE, Hollan I, Feinberg MW, et al. Antirheumatic therapy is associated with reduced complement activation in rheumatoid arthritis. *PloS One*. (2022) 17:e0264628. doi: 10.1371/journal.pone.0264628

76. Trouw LA, Pickering MC, Blom AM. The complement system as a potential therapeutic target in rheumatic disease. *Nat Rev Rheumatol*. (2017) 13:538–47. doi: 10.1038/nrrheum.2017.125

77. Yasutomi Y, Chiba A, Haga K, Murayama G, Makiyama A, Kuga T, et al. Activated mucosal-associated invariant T cells have a pathogenic role in a murine model of inflammatory bowel disease. *Cell Mol Gastroenterol Hepatol*. (2022) 13:81–93. doi: 10.1016/j.jcmgh.2021.08.018

78. Chiba A, Murayama G, Miyake S. Characteristics of mucosal-associated invariant T cells and their roles in immune diseases. *Int Immunol*. (2021) 33:775–80. doi: 10.1093/intimm/dxab070

79. Sun X, Nguyen T, Achour A, Ko A, Cifello J, Ling C, et al. Longitudinal analysis reveals age-related changes in the T cell receptor repertoire of human T cell subsets. *J Clin Invest*. (2022) 132(17):e158122. doi: 10.1172/JCI158122

80. Zhang H, Weyand CM, Goronzy JJ. Hallmarks of the aging T-cell system. *FEBS J*. (2021) 288:7123–42. doi: 10.1111/febs.v288.24

81. Kaplan SA. Factors in predicting failure with medical therapy for BPH. *Rev Urol*. (2005) 7 Suppl 7:S34–9.

82. Mehrotra R, Pandya S, Singhla M, Srivastava D, Singh M. Spectrum of Malignancies in Allahabad, North India: a hospital-based study. *Asian Pac J Cancer Prev*. (2008) 9:525–8.

83. Moller M, Strand SH, Mundbjerg K, Liang G, Gill I, Haldrup C, et al. Heterogeneous patterns of DNA methylation-based field effects in histologically normal prostate tissue from cancer patients. *Sci Rep*. (2017) 7:40636. doi: 10.1038/srep40636